Journal of Cell Science 111, 1363-1370 (1998)
Printed in Great Britain © The Company of Biologists Limited 1998
JCS3697

Clustering of pericentromeres initiates in step 9 of spermiogenesis of the rat (*Rattus norvegicus*) and contributes to a well defined genome architecture in the sperm nucleus

Mirella Meyer-Ficca[1], Jutta Müller-Navia[2] and Harry Scherthan[1,3,*]

[1]Abt. für Humanbiologie, Universität Kaiserslautern, Postf. 3049, D-67653 Kaiserslautern, Germany
[2]Inst. für Anthropologie und Humangenetik der Universität, Saarstr.21, D-55122 Mainz, Germany
[3]Abt. für Zellbiologie, Universität Kaiserslautern, Postf. 3049, D-67653 Kaiserslautern, Germany
*Author for correspondence (e-mail: scherth@rhrk.uni-kl.de)

Accepted 23 February; published on WWW 29 April 1998

SUMMARY

Fluorescence in situ hybridization with centromeric, telomeric and whole chromosome paint probes was used to study nuclear topology in epididymal sperm as well as spermatids from testis tissue sections of the rat. Pericentromeric regions of 9 chromosomes of the rat (*n*=21) were labeled with a satellite I specific DNA probe. Pericentromeres showed few tandem associations in spermatids of steps 1-8 of spermiogenesis. At step 9, pericentromeric regions associated to form an elongated cluster in the spermatid nucleus. This arrangement was also seen in the sperm nucleus. FISH with telomere probes revealed numerous, variably arranged signals in round and elongated spermatids as well as sperm nuclei. Telomere signals showed a tendency for pairwise association which was more pronounced in elongated spermatid and epididymal sperm nuclei. FISH to DTT treated sperm suggested that telomeres reside at the periphery and that pericentromeres are located in the nuclear interior. Chromosome painting with rat chromosome 2 and 12 specific microdissection library probes showed that these chromosomes predominantly occupy compact and variably shaped territories during spermatid maturation. In elongated epididymal sperm nuclei chromosome 2 and 12 territories took up specific positions. We suppose that the associations of pericentromeres during step 9 render a well defined nuclear topology which facilitates the ordered compaction of the genome at subsequent stages.

Key words: Fluorescence in situ hybridization, Sperm head, Nuclear architecture, Spermiogenesis, Satellite DNA, Centromere, Telomere, Chromosome painting, Rat

INTRODUCTION

The arrangement of chromosomes at interphase has been an intensively studied issue for more than a century. It is now well acknowledged that chromosomes at interphase are organized in territories and display a cell type specific distribution (for review see Heslop-Harrison and Bennett, 1990; Haaf and Schmid, 1991; Cremer et al., 1993; Marshall et al., 1997). Recently, is has been shown that the architecture of the mammalian sperm nucleus is highly organized (Zalensky et al., 1993, 1995; Haaf and Ward, 1995). During spermatid differentiation nuclear chromatin is reorganized from nucleosomal packaging to a tightly condensed and transcriptionally inactive protamine form (Kierszenbaum and Tres, 1975; Loir and Courtens 1979; Kistler et al., 1996). Moreover, it has been demonstrated that centromeres and telomeres exhibit specific associations in the sperm nucleus (Haaf et al., 1990; Zalensky et al., 1993, 1997; Watson et al., 1996). Different centromere distribution patterns in early and late mouse spermatids suggest that nuclear topology is reorganized during spermiogenesis (Brinkley et al., 1986). Although nuclear architecture in human and mouse sperm has been studied in great detail, it has remained enigmatic when during spermiogenesis this reorganization occurs.

Since rat sperm heads display a unique elongated morphology and rat spermiogenesis is well characterized (Leblond and Clermont, 1952; Clermont and Harvey, 1965; Hess, 1990), we have investigated the nuclear organization in sperm of the rat (*Rattus norvegicus*) by fluorescence in situ hybridization (FISH) with centromere, telomere and whole chromosome paint probes. This analysis revealed that pericentromeric satellite DNA forms large elongated aggregates, while chromosomes are non-randomly distributed in the oblong sperm nucleus. FISH to DDT treated sperm nuclei suggested that telomeres occupy a peripheral position, while satellite DNA is more internally located. FISH to formaldehyde fixed rat testis sections demonstrated that clustering of pericentromeric satellite DNA commences in step 9 of rat spermiogenesis, while a significant reduction of telomere signals was observed at step 10.

MATERIALS AND METHODS

Cell cultures and chromosome preparation

A *Rattus norvegicus* fibroblast cell line was obtained from fetal rat tissue (Kappler et al., 1997). Cells were cultured in EMEM supplemented with 10% FCS (both Life technologies). Colchicine arrested fibroblasts were swollen in 0.05 M KCl for 30 minutes at 37°C and fixed overnight with freshly prepared ice-cold methanol/acetic acid (3/1). Chromosome preparations were obtained as described (Kappler et al., 1998).

Tissue origin and processing

Male Wistar rats were killed and the testes resected. The epididymes were removed and testes were instantly frozen in liquid nitrogen. Epididymal sperm preparations were obtained as described (Watson et al., 1996). In some experiments sperm heads were decondensed by a 10 minute incubation in 50 mM DTT, 50 mM KCl at 37°C.

10 μm sections were cut from frozen testis tissue using a cryomicrotome (Jung), bound to glass slides (Superfrost Plus, Menzel Gläser) and subsequently fixed in phosphate buffered formaldehyde (4%) for 25 minutes. Sections were rinsed in PBS prior to further processing.

DNA probes and labeling

The pericentromeric heterochromatin of 18 rat chromosomes was delineated with a 5′ fluorescein labeled rat satellite I-specific 42mer oligonucleotide probe (*RS1*: 5′-CTGAAACACT GTTTCTTTGT GAATTCAGTT AGTTCCTTCT AG-3′; Scherthan and Cremer, 1994) (Fig. 1). $(TTAGGG)_7$ and $(CCCTAA)_7$ oligonucleotide probes (Moyzis et al., 1988; Scherthan, 1990) were used to label rat telomeres (not shown).

Rat chromosome (RNO) 2 and 12 specific whole chromosome paint probes (WCP) (see Fig. 8) were generated by microdissection of the respective chromosomes and subsequent amplification by DOP-PCR (Müller-Navia et al., 1995). RNO 2 and 12 WCPs were labeled with biotin-14-dATP (life technologies) or digoxigenin-11-dUTP (Boehringer) using a random priming kit according to the instructions of the manufacturer (life technologies). Labeled chromosome specific library DNA was ethanol precipitated in the presence of a 25-fold excess of rat C_0t-1 DNA. The latter was prepared from genomic rat DNA according to Kappler et al. (1998).

In situ hybridization to tissue sections and probe detection

Prior to FISH, formaldehyde fixed tissue sections were digested for 1 hour at 37°C with RNase A (Sigma; 200 μg/ml 2× SSC). Preparations were rinsed with deionized water and excess liquid was drained from the sections. 2.5 μl of hybridization solution (see Scherthan and Cremer, 1994) was applied per slide and sealed under a 14 mm ×14 mm coverslip. After denaturation for 5 minutes at 83°C, hybridization was carried out for 64 hours. Post-hybridization washes and probe detection were carried out as described previously (Scherthan and Cremer, 1994). After detection preparations were embedded in antifade solution (Vector) which contained 1 μg/ml DAPI (4,6-diamidino-2-pheylindole) as DNA-specific counterstain.

FISH to sperm heads

Sperm preparations were submersed for 1 hour in 1 M NaSCN (Hopman et al., 1991) at 73°C. Preparations were then incubated in 50% formamide/2× SSC for 2 minutes at 80°C, followed by incubation at 37°C for 12 hours and another 2 minutes at 80°C. Slides were rinsed, dried and previously denatured hybridization solution was added and sealed under a coverslip. Hybridization was performed for 48 hours and detection of hybrid molecules was performed as described (Scherthan and Cremer, 1994). This procedure resulted in well preserved sperm morphology and strong hybridization signals.

Light microscopic evaluation and image recording

Preparations were evaluated using a Zeiss Axioskop epifluorescence microscope equipped with single band pass filters for excitation of blue, green and red fluorescence (Chroma Technologies). Digital black-and-white images were recorded with a cooled CCD camera (Hamamatsu) and merged to rgb-images by the ISIS fluorescence image analysis system (MetaSystems). For display color images were converted into gray scale images.

RESULTS

Rat sperm nuclei display prominent clustering of pericentromeric heterochromatin

FISH with the rat satellite I oligonucleotide probe rendered strong signals at the pericentromeric region of 18 out of the 42 rat chromosomes (Fig. 1). FISH to epididymal sperm preparations pretreated with sodium thiocyanate and sequential heat denaturation resulted in strong signals in morphologically well preserved rat sperm nuclei. Within these, pericentromeres were predominantly distributed in oblong clusters along the

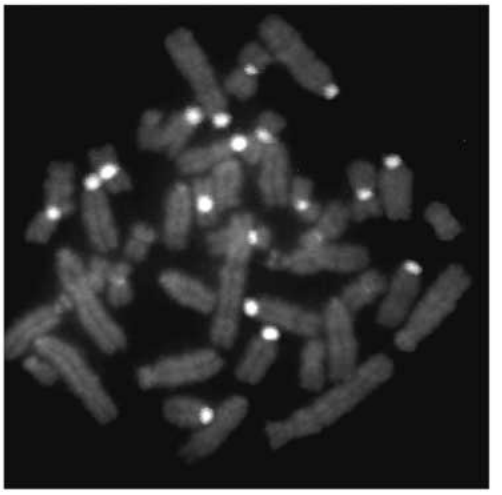

Fig. 1. Rat metaphase chromosomes hybridized with the satellite DNA specific, fluorescein labeled oligonucleotide probe. Prominent signals (whitish) are apparent at 18 centromeres.

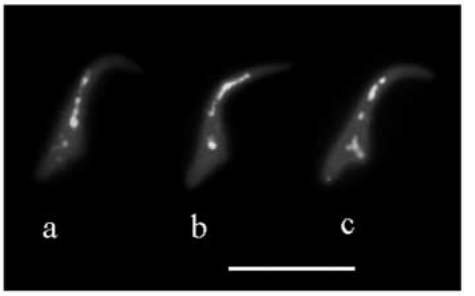

Fig. 2. FISH with pericentromeric rat satellite DNA to nuclei from epididymal sperm suspensions. Typical signal patterns are shown. (a) Pericentromeric satellite DNA forms an oblong continuous signal cluster along the median region of the sperm nucleus. (b) An elongated signal is seen apically and a single cluster is seen in the median part of the sperm nucleus. (c) Five signal clusters are seen along the longitudinal axis of the nucleus. Bar, 15 μm.

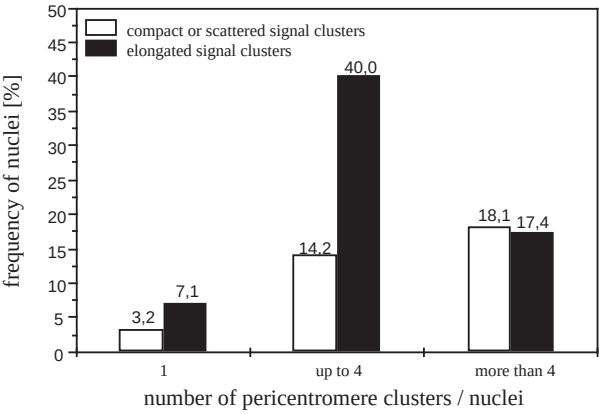

Fig. 3. Number and shape of pericentromere signals in sperm nuclei (*n*=155).

longitudinal axis of the nucleus (Fig. 2). Nuclei with compacted, more or less round signal clusters were observed at a significantly lower frequency. Pericentromeric signals tended to associate in groups, a signal arrangement which was designated as 'locally clustered' (Fig. 3). Swelling of sperm nuclei by additional DTT or detergent treatment perturbed nuclear morphology and led to the disintegration of the single, oblong satellite DNA clusters into few large signals (not shown). This is consistent with earlier observations (Moens and Pearlman, 1989). DDT pretreatment did also release peripheral chromatin from the sperm nucleus. Satellite signals, however, were always confined to the DAPI bright nuclear mass.

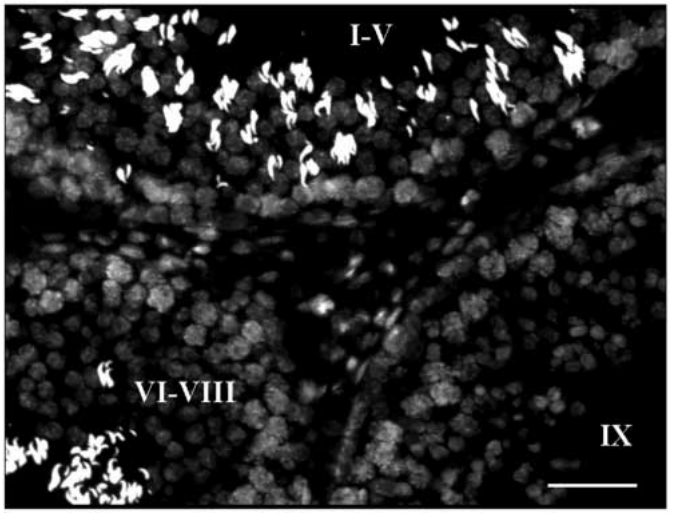

Fig. 4. Overview of a DAPI stained testis tissue section after in situ hybridization. The stages of the seminiferous epithelium are indicated by the roman numbers. Where stages could not unequivocally be identified these were included in a common category (i.e. I-V and VI-VIII; for details see text). Elongated spermatids in the two tubuli to the left show intense fluorescence. They are embedded in round spermatids in the stage I-V tubule, while they are seen near the lumen of the VI-VIII tubule. The stage IX tubule shows round spermatids in the adluminal region. Bar, 50 μm.

Pericentromere distribution in step 1-8 spermatids

Previous FISH analysis of rat spermatogenetic cells from spread preparations demonstrated a dispersed arrangement of pericentromeres in round spermatids (Moens and Pearlman, 1989). Since we detected prominent centromere clustering in mildly swollen sperm nuclei, we wished to test at which step of spermiogenesis centromere clustering occurred. To this end, FISH with the rat satellite DNA probe to formaldehyde fixed testis tissue sections was performed. The histological context of DAPI-stained sections was exploited to identify particular stages of the seminiferous epithelium of testis tubuli (Fig. 4). In the rat this highly specialized epithelium can be subdivided into 14 stages, while 19 steps of spermiogenesis can be distinguished according to spermatid morphology (Leblond and Clermont, 1952; Hess, 1990). In the present analysis we pooled round spermatids of steps 1-5 and of steps 6-8 as two individual categories, since the pretreatment for FISH led to loss of cytoplasm. Tissue sections, therefore, did not reveal the subtle morphological differences of round spermatids needed for further subdivision of these stages. However, testis tubuli at stages IX–XIV of the seminiferous epithelium and by this spermatids of steps 9-14 could be identified according to the

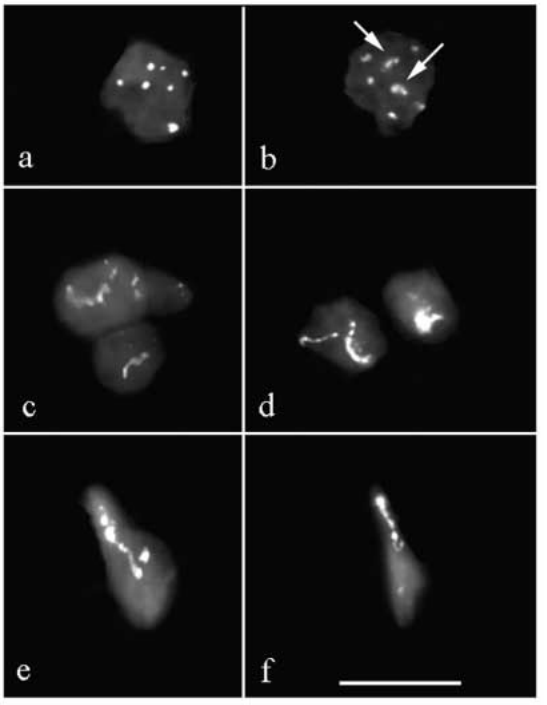

Fig. 5. Round spermatids taken from different testis tubuli after FISH with the FITC-labeled pericentromeric satellite DNA probe (whitish). (a) A step 1-5 spermatid exhibits 7 round pericentromeric satellite signals. (b) Step 6-8 spermatid with 7 pericentromeric signals. Two signal pairs near the nuclear center show tandem association (arrows). (c) Step 9 spermatids exhibit a conspicuous necklace like association of pericentromeric signals. (d) Step 10 spermatids. The leftmost displays a necklace-like association of pericentromeric signals, while the other exhibits one compact satellite cluster. (e) An elongated step 11-12 spermatid shows a linear arrangement of clustered pericentromeres. (f) Step 13-14 spermatid with oblong satellite signal cluster in the apical nuclear region. Bar in f, 15 μm.

differences in the morphology of the elongating rat spermatid nucleus (Leblond and Clermont, 1952; see Fig. 4).

Satellite-DNA FISH experiments to tissue sections disclosed 4 to 8, generally round, pericentromeric signals in spermatids of steps 1–5 (Figs 5, 6a). In a fraction of these cells the signal number nearly reached the theoretical 9 signals which are expected if pericentromeres were distributed independently in the haploid spermatid nucleus.

In spermatids of steps 6-8 signal distribution was similar as compared to steps 1-5. However, a minor fraction of nuclei appeared which showed a tendency of local pericentromere clustering (Fig. 6b). Local clustering was defined when signals were not separated by more than their diameter (Fig. 5b).

Pericentromere redistribution initiates prior to spermatid elongation

A drastic shift in signal arrangement was observed in step 9 spermatids. At this step pericentromeric signals generally formed thin and oblong clusters (Fig. 5c). The predominant signal pattern was 1 elongated cluster per nucleus, while other patterns were seen at low frequencies (Fig. 6c).

The elongation of the spermatid nucleus commences at step 10 (Leblond and Clermont, 1952; Clermont and Harvey, 1965; Hess, 1990). Among spermatids of steps 10-12 and of steps 13-14 the frequency of nuclei with single elongated clusters of pericentromeric satellite DNA (Fig. 5d-f) increased further (Fig. 6d,e). Elongated spermatid nuclei with dispersed satellite signals were not observed (Fig. 6e).

Spermatids of steps 15-19 did not display FISH signals, which most likely relates to high chromatin compaction that prevents access of the probe to the only mildly pretreated spermatids in tissue sections.

Telomere distribution in spermiogenic nuclei

To investigate telomere distribution in differentiating spermatids and epididymal sperm nuclei we performed FISH with a biotinylated $(TTAGGG)_7$ DNA probe, which in the rat exclusively labels telomeric sequences at chromosome ends (Moyzis et al., 1988). FISH with these telomere probes to spermatids from testis tissue sections revealed dot-like signals of variable intensity and distribution in spermatid and sperm nuclei (Fig. 7). Pairwise associations of telomere signals were observed in spermatids of various steps of development and were more pronounced in elongating spermatids (Fig. 7d-f) and sperm nuclei (Fig. 7g,h).

An increase in telomere associations in the more advanced steps is reflected by reduced signal numbers/nucleus in step 10-

Table 1. Mean telomere signal number/nucleus at various steps of spermatid differentiation

Steps of spermatid differentiation	Mean telomere signal no. (±s.d.)*
1-8	28 (±5.4)
9	27.3 (±4.7)†
10	21.9 (±4.5)†
11-12	20.5 (±3.4)
13-14	19.4 (±3.6)

*50 nuclei were evaluated for each category.

†Telomere signal numbers differ highly significantly (P<0.001) between steps 9 and 10.

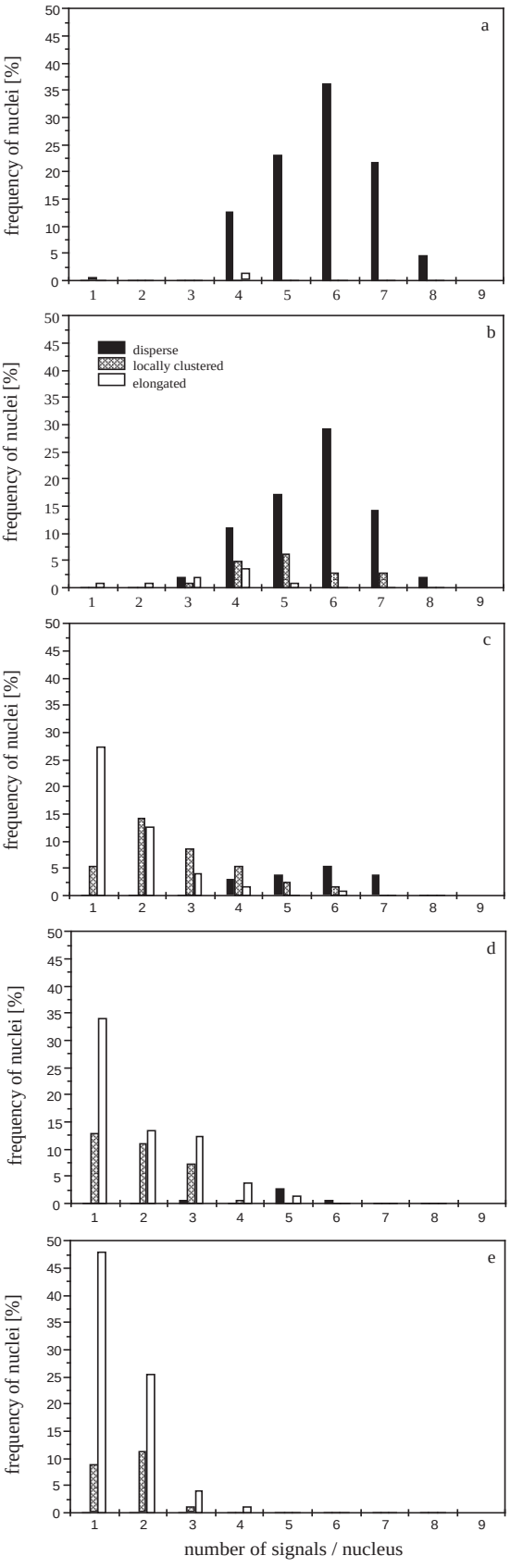

Fig. 6. Distribution and morphology of pericentromere signals in spermatids of: (a) steps 1-5 (n=152); (b) steps 6-8 (n=47); (c) step 9 (n=128); (d) steps 10-12 (n=156); and (e) steps 13-14 (n=248).

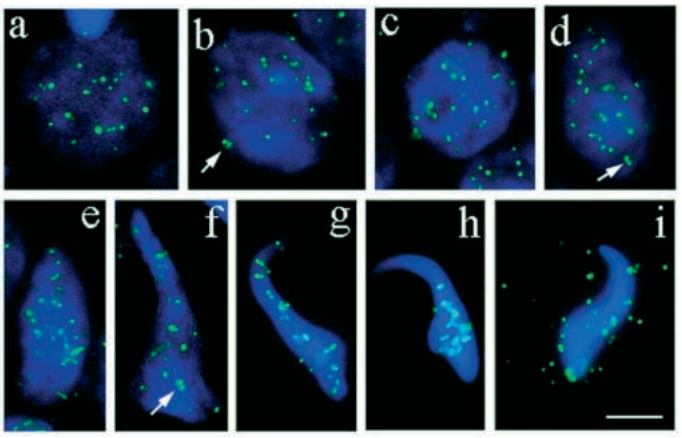

Fig. 7. Representative images of FISH with $(TTAGGG)_7$ telomere DNA probes (green) to spermatids from rat testis sections at steps (a) 4-7, (b) 8, (c) 9, (d,e) 10, and (f) 12 of spermiogenesis and to (g,h) sperm nuclei. Telomere signals are seen as bright spots which are sometimes associated in pairs (arrows in b,d,f). Telomere signal dimers and signal associations are pronounced in epididymal sperm (g,h). (i) Telomere signals surround a sperm nucleus after DTT treatment. DNA was counterstained with DAPI. Bar, 5 μm.

14 spermatids as compared to step 1-9 spermatids (Table 1). While signal numbers did not differ significantly between steps 1-8 and 9 a highly significant drop (P<0.001) of signal numbers was observed between step 9 and step 10 (Table 1). Mean signal numbers for steps 10 and 11-12 were similar, but a significant reduction in telomere signals (P<0.05) was apparent between step 10 and step 13-14 spermatids.

Telomere signals in epididymal sperm nuclei were often of rod like morphology or showed associations in pairs or multiples thereof (Fig. 7). The mean signal number per nucleus was 17 (16.9±3.8). Most signals located in the median-basal region of the sperm nucleus, but few signal pairs were consistently seen in the apical part of nuclei (Fig. 7g). Nuclei which showed all telomere signals exclusively concentrated in the median-basal part of the nucleus (Fig. 7h) were observed at a low frequency (5%; n=117).

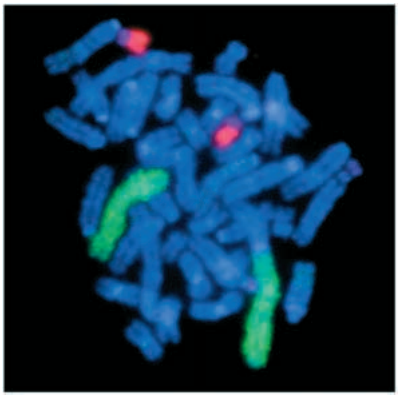

Fig. 8. Rat metaphase spread hybridized with the chromosome 2 specific (fluorescein, green) and the chromosome 12 specific (rhodamine, red) labeled microdissection whole chromosome paint probes. The weak staining of RNO 12p results from the suppression of the NOR at this location.

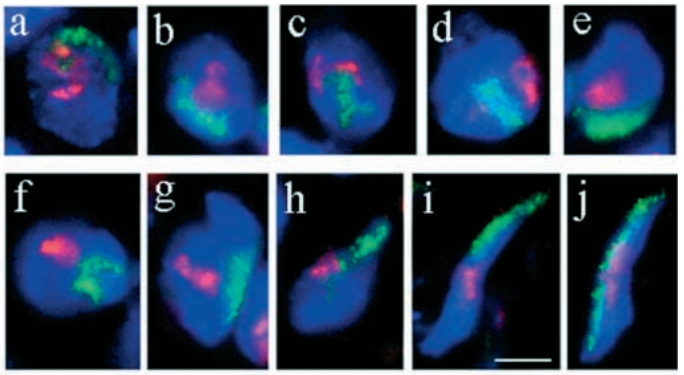

Fig. 9. Representative images of chromosome painting in spermatids of steps (a) 7, (b) 8, (c,d) 9, (e-g) 10, (h) 11, and (i,j) 13 of spermiogenesis. RNO2 chromosome territories of (green, FITC) are oblong and variably shaped. In spermatids of step 13 RNO2 territories stretch along the longitudinal axis of the nucleus. RNO12 (red, rhodamine) occupies smaller territories of variable shape. In step 13 spermatids (i,j) its signal occupies a median position. DNA was counterstained with DAPI (blue). Bar, 5 μm.

It has been proposed that telomeres locate at the nuclear periphery of the mammalian sperm nucleus (Zalensky et al., 1993, 1997; Haaf and Ward, 1995). Since peripherally located telomeres can be released from the nuclear mass by DTT and/or heparin treatment (see Zalensky et al., 1997), we incubated epididymal rat sperm in 50 mM DTT/KCl solution. This treatment induced swelling of the nuclei and released peripheral chromatin from the DAPI bright nuclear mass. In such nuclei telomere signals were dispersed over and around the nucleus (Fig. 7i), which indicates a peripheral location of telomeres in rat sperm nuclei.

Chromosomes are preferentially distributed in the rat sperm nucleus

Clustering of interior pericentromeres and associations of peripheral telomeres suggested an ordered organization of chromosomes in rat sperm. To investigate the positioning of whole chromosomes in spermatids and in sperm nuclei, we generated WCPs specific for RNO2 and RNO12 by microdissection. RNO2 represents a large acrocentric chromosome, while RNO12 is a medium sized submetacentric chromosome with a NOR situated in its short arm. Chromosome painting on metaphase spreads showed a high specificity of the two microdissection probes (Fig. 8). Since the

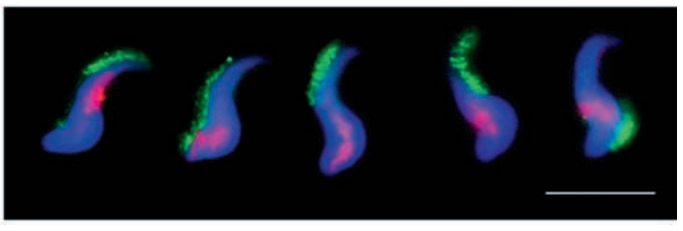

Fig. 10. Two color FISH with RNO2 (green) and RNO12 (red) specific WCPs to rat sperm nuclei. RNO2 signals frequently extend between the median and either apical or basal part of the sperm head. RNO12 is predominantly located in the median region of the nucleus (see Fig. 11). DNA was counterstained with DAPI (blue). Bar, 15 μm.

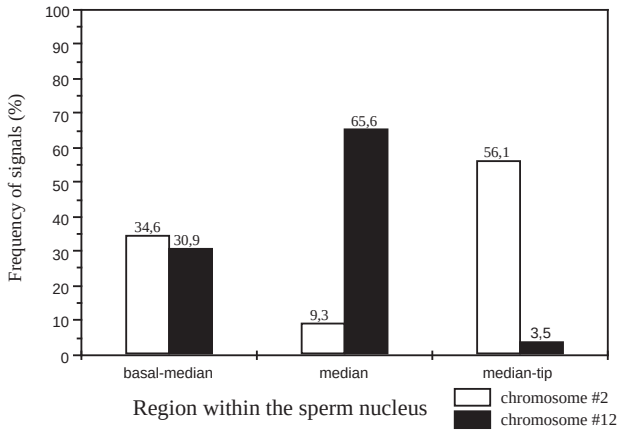

Fig. 11. Distribution of RNO2 and 12 signals in the sperm nucleus (*n*=302).

C_0t-1 DNA in the hybridization solution suppressed hybridization of repetitive DNA sequences, the short arm of RNO12 (due to its NOR) was only weakly labeled as compared to its long arm. In experiments with low amounts of suppression DNA RNO12p was brightly labeled but signals were also seen at the NORs of RNO3 and 11 (not shown), which is consistent with the location of 3 NORs in the haploid rat complement (Kano et al., 1976).

Chromosome painting with both WCPs to rat testis tissue sections revealed that the large chromosome 2 territory was predominantly of compact morphology, while chromosome 12 territories were more variably shaped in step 1–10 spermatids (Fig. 9). In elongating spermatids of steps 11–13 the RNO2 territory primarily extended along the longitudinal axis of the nucleus (Fig. 9h-j), while RNO12 preferentially occupied a median position. In epididymal sperm nuclei chromosome territories were generally of rod-like morphology (Fig. 10) and chromosome distribution was not random: Like in step 11 and 13 spermatids, extended RNO12 signals were predominantly located in the median region, while the threadlike RNO2 signals primarily stretched between the median region and the tip or basal region of the sperm head (Figs 10, 11).

DISCUSSION

Architecture of the rat sperm nucleus

It has been shown that the pairwise and multiple association of kinetochores imposes some type of order to mammalian sperm nuclear architecture (Brinkley et al., 1986; Haaf et al., 1990; Zalensky et al., 1993). Chromatin packaging in the sperm nucleus is sequence specific (Gatewood et al., 1987) and it has been shown that pericentromeric heterochromatin forms large central clusters in mammalian sperm (Powell et al., 1990; Zalensky et al., 1993, 1995; Haaf and Ward, 1995).

In the oblong rat sperm nucleus we also observed large elongated clusters of pericentromeric satellite DNA. Although considerable differences in morphology exist between mouse, human and rat sperm, these obviously display a conserved nuclear topology. Like in mouse (Haaf and Ward, 1995) and human (Zalensky et al., 1993), whole chromosomes preferentially occupy elongated threadlike territories within the rat sperm head. It has been hypothesized that internal centromere clustering and peripheral telomere associations impose a structural framework on genome topology in mammalian sperm (Zalensky et al., 1995; Haaf and Ward 1995). Distinct oblong pericentromere clusters were observed along the longitudinal axis of the rat sperm nucleus. These are most likely located in the nuclear interior, since satellite signals were never observed in the peripheral chromatin fraction released by DTT treatment. Telomeres, on the other hand, are most likely peripherally located, since this treatment dissociated telomere signals from the nuclear mass. In mildly treated rat sperm, telomere signals were often associated in dimers. These associations may explain why we never observed a signal number corresponding to the number of chromosome ends of the haploid rat complement (i.e. 42 telomeres). The majority of telomeres concentrated in the median-basal region of the nucleus (Zalensky et al., 1997; this investigation). This concentration may be the consequence of the clustering of the centromere proximal telomeres of acrocentric chromosomes at the chromocenter and the preferential location of the smaller chromosomes in the wider basal part of the rat sperm nucleus (see below). It appears that specific arrangement of centromeres and telomeres is an intrinsic part of the nuclear organization of the highly differentiated rat sperm nucleus and resembles the nuclear organization of other mammalian sperm (Haaf and Ward, 1995; Zalensky et al., 1997).

Whole chromosomes occupy specific positions in the rat sperm nucleus

In spermatids up to step 10 of spermiogenesis, RNO2, which is a large acrocentric chromosome, and the smaller RNO12 predominantly adopted compacted territories of variable shape. In elongated spermatids and epididymal sperm, RNO2 territories were of rod-like shape and generally extended between the median region and the apical or basal part of the sperm head. Threadlike chromosome territories have also been observed in mouse and human sperm (Haaf and Ward, 1995). Since the centromeric heterochromatin cluster located predominantly in the median region of the sperm nucleus and since few telomere signals were seen in the nuclear tip of 95% of rat sperm investigated, it may be assumed that the acrocentric RNO2 stretches between a basally located centromere and an apically located telomere. However, RNO2 specific telomere and centromere DNA probes are required to finally resolve this question, since the pericentromere of RNO2 is not delineated by the satellite DNA probe applied.

In contrast to RNO2, the smaller chromosome 12 occupied a more central location in the rat sperm head. This arrangement is probably a consequence of its smaller physical size and the preferential location of its centromere in the median region of the nucleus. The median location of RNO12 could also relate to a non-random NOR positioning, since it has been observed that NORs in mouse and cattle sperm tend to associate with the chromocenter in the central region of the nucleus (Powell et al., 1990; Haaf and Ward, 1995). It can be expected that the generation of more WCPs suitable for rat interphase chromosome painting will further refine the image of nuclear architecture of the sperm head.

Strong evidence of non-random arrangement of chromosomes in sperm nuclei has been obtained in species in

which the sperm head displays a threadlike morphology (Hughes-Schrader, 1946; Inoue and Sato, 1962; Watson et al., 1996). Since chromosomes seem to be tandemly arranged and tend to occupy a fixed position in filamentous monotreme sperm nuclei (Watson et al., 1996), it appears that basic motifs of the organization of the paternal complement in this specialized cell type have been highly conserved throughout mammalian evolution.

Pericentromere clustering initiates during step 9 of spermiogenesis

Different distribution patterns of pericentromeres have been observed in rat spermatids (Moens and Pearlman, 1989) and epididymal sperm (this investigation). To address the question when during spermatid differentiation centromere regrouping occurs, we stained rat pericentromeric satellite DNA by FISH to testis tissue sections and analyzed spermatids at various steps of spermiogenesis. It was found that spermatids of steps 1-8 predominantly exhibited 4-8 pericentromeric signals, which suggests that pericentromeres are distributed separately and in a few tandem associations during these early steps of spermiogenesis. At step 9 of rat spermiogenesis a drastic redistribution of pericentromeric satellite DNA clusters was observed (Fig. 5). This redistribution seems to be a rather rapid process, since steps 9-11 take roughly one day (Clermont and Harvey, 1965; Meistrich et al., 1989). The number of spermatids which showed a single pericentromere cluster further increased concomitantly with the elongation of the rat spermatid nucleus during steps 10-14. Step 15-19 spermatids from testis tissue sections did not show FISH signals due to the high chromatin compaction at these steps. However, in epididymal sperm heads satellite clusters were more numerous than in spermatids of steps 12-14. This discrepancy is most likely a consequence of the mild swelling of the sperm nuclei prior to FISH, since in tissue section FISH experiments this step was omitted to preserve spermatid morphology.

Telomere arrangement during spermatid development

Since telomeres in sperm nuclei tend to associate in dimers and multiples thereof (see Zalensky et al., 1997), we also investigated telomere distribution in rat spermatids at various steps of development. While spermatids of steps 1-8 and 9 displayed similar telomere signal numbers, mean signal numbers progressively reduced in elongating spermatids of steps 10-14 (Table 1). It can be expected that the telomere signal numbers observed in spermatids and sperm are overestimations, since telomere associations are likely disrupted to some extent by the pretreatments and denaturation of the nuclear chromatin. In spite of these limitations we observed a highly significant reduction of telomere signal numbers between steps 9 and 10 of spermiogenesis, which suggests that from step 10 on further telomere associations are established. According to this timing these follow centromere clustering which initiates at step 9 and may act as a nucleation point for alteration of genome architecture during spermatid differentiation.

At step 9 of spermiogenesis the initiation of chromatin reorganization is reflected by the appearance of initial amounts of the spermatid specific transition protein 2 (Kistler et al., 1996; Oko et al., 1996). The commencement of pericentromere association during step 9 suggests that chromosome topology is altered prior to fibrillar chromatin condensation, which occurs during steps 11-13 (Oko et al., 1996). It has been speculated that nuclear architecture and interphase chromosome distribution is linked to the transcriptional activity of a cell or cell type (for review see e.g. Cremer et al., 1993; Strouboulis and Wolffe, 1996). Decline of transcriptional activity could therefore pave the way for compression of chromosome territories and thereby the ordered compaction of the genome during spermiogenesis.

This work was supported in part by the Deutsche Forschungsgemeinschaft (Sche 350/8-1).

REFERENCES

Brinkley, B. R., Brenner, S. L., Hall, J. M., Tousson, A., Balczon, R. D. and Valdivia M. M. (1986). Arrangement of kinetochores in mouse cells during meiosis and spermiogenesis. *Chromosoma* **94**, 309-317.

Clermont, Y. and Harvey, S. C. (1965). Duration of the cycle of the seminiferous epithelium of normal hypophysectomized and hypophysectomized hormone treated albino rats. *Endocrinology* **76**, 80-89.

Cremer, T., Kurz, A., Zirbel, R., Dietzel, S., Rinke, B., Schröck, E., Speicher, M. R., Mathieu, U., Jauch, A., Emmerich, P., Scherthan, H., Cremer, C. and Lichter, P. (1993). Role of chromosome territories in the functional compartmentalization of the cell nucleus. *Cold Spring Harbor Symp. Quant. Biol.* **58**, 777-792.

Gatewood, J. M., Cook, G. R., Balhorn, R., Bradbury, E. M. and Schmid, C. W. (1987). Sequence-specific packaging of DNA in human sperm chromatin. *Science* **236**, 962-964.

Guttenbach, M. and Schmid, M. (1990). Determination of Y chromosome aneuploidy in human sperm nuclei by nonradioactive in situ hybridization. *Am. J. Hum. Genet.* **46**, 553-558.

Haaf, T., Grunenberg, H. and Schmid, M. (1990). Paired arrangement of nonhomologous centromeres during vertebrate spermiogenesis. *Exp. Cell Res.* **187**, 157-161.

Haaf, T. and Schmid, M. (1991). Chromosome topology in mammalian interphase nuclei. *Exp. Cell Res.* **192**, 325-332.

Haaf, T. and Ward, D. C. (1995). Higher order nuclear structure in mammalian sperm revealed by *in situ* hybridisation and extended chromatin fibers. *Exp. Cell Res.* **219**, 604-611.

Hess, R. A. (1990). Quantitative and qualitative characteristics of the stages and transitions in the cycle of the rat seminiferous epithelium: light microscopic observations of the perfusion-fixed and the plastic-embedded testes. *Biol. Reprod.* **43**, 525-542.

Heslop-Harrison, J. S. and Bennett, M. D. (1990). Nuclear architecture in plants. *Trends Genet.* **6**, 401-405.

Hopman, A. H. N., van Hooren, E., van de Kaa, Ch. A., Vooijs, P. G. P. and Ramaekers F. C. S. (1991). Detection of numerical chromosome aberrations using in situ hybridization in paraffin sections of routinely processed bladder cancers. *Modern Pathol.* **4**, 503-513.

Hughes-Schrader, S. (1946). A new type of spermiogenesis in icerine coccids, with linear arrangement of chromosomes in the sperm. *J. Morphol.* **78**, 43-77.

Inoue, S. and Sato, H. (1962). Arrangement of DNA in living sperm: a biophysical analysis. *Science* **136**, 1122-1124.

Kano, Y., Maeda, S. and Sugiyama, T. (1976). The location of ribosomal cistrons (rDNA) in chromosomes of the rat. *Chromosoma* **55**, 37-42.

Kappler, R., Schlegel, J., Romanakis, K., Mennel, H. D. and Scherthan, H. (1998). Comparative genomic in situ hybridization discloses chromosomal copy number changes in a transplanted brain tumor line of the rat (*Rattus norvegicus*). *Mammalian Genome* **9**, 193-197.

Kierszenbaum, A. L. and Tres, L. L. (1975). Structural and transcriptional features of the mouse spermatid genome. *J. Cell Biol.* **65**, 258-270.

Kistler, W. S., Henriksén, K., Mali, P. and Parvinen, M. (1996). Sequential expression of nucleoproteins during rat spermiogenesis. *Exp. Cell Res.* **225**, 374-381.

Leblond, C. P. and Clermont, T. Y. (1952). Definition of the stages of the cycle of the seminiferous epithelium in the rat. *Ann. NY Acad. Sci.* **55**, 548-573.

Loir, M. and Courtens, J. L. (1979). Nuclear reorganization in ram spermatids. *J. Ultrastruct. Res.* **67**, 309-324.

Marshall, W. F., Fung, J. C. and Sedat, J. W. (1997). Deconstructing the nucleus: global architecture from local interactions. *Curr. Opin. Genet. Dev.* **7**, 259-263.

Meistrich, M. L., Trostle-Weige, P. K. and Van Beek, M. E. (1989). Separation of specific stages of spermatids from vitamin A-synchronized rat testes for assessment of nucleoprotein changes during spermiogenesis. *Biol. Reprod.* **51**, 334-344.

Moens, P. B. and Pearlman, R. E. (1989). Satellite DNA I in chromatin loops of rat pachytene chromosomes and in spermatids. *Chromosoma* **98**, 287-294.

Moyzis, R. K., Buckingham, J. M., Cram, C. S., Dani, M., Deaven, L. L., Jones, D. J., Meyne, J., Ratcliff, R. L. and Wu, J. R. (1988). A highly conserved DNA sequence, $(TTAGGG)_n$ present at the telomeres of human chromosomes. *Proc. Nat. Acad. Sci. USA* **85**, 6622-6628.

Müller-Navia, J., Nebel, A. and Schleiermacher, E. (1995). Complete and precise characterization of marker chromosomes by application of microdissection in prenatal diagnosis. *Hum. Genet.* **96**, 661-667.

Oko, R. J., Jando, V., Wagner, C. L., Kistler, W. S. and Hermo, L. S. (1996). Chromatin reorganization in rat spermatids during the disappearance of testis-specific histone, H1t, and the appearance of transition proteins TP1and TP2. *Biol. Reprod.* **54**, 1141-1157.

Powell, D., Cran, D. G., Jennings, C. and Jones, R. (1990). Spatial organization of repetitive DNA sequences in the bovine sperm nucleus. *J. Cell Sci.* **97**, 185-191.

Scherthan, H. (1990). Localization of the repetitive telomeric sequence $(TTAGGG)_n$ in two muntjac species and implications for their karyotypic evolution. *Cytogenet. Cell Genet.* **53**, 115-117.

Scherthan, H. and Cremer, T. (1994). Methodology of non-isotopic in situ hybridisation in paraffin embedded tissue sections. In *Methods in Molecular Genetics*, vol. 5, *Chromosome and Gene Analysis* (ed. K. W. Adolph), pp. 223-238. Academic Press, San Diego.

Strouboulis, J. and Wolffe, A. P. (1996). Functional compartmentalization of the nucleus. *J. Cell Sci.* **109**, 1991-2000.

Watson, J., Meyne, J. and Graves, J. A. M. (1996). Ordered tandem arrangement of chromsomes in the sperm heads of monotreme mammals. *Proc. Nat. Acad. Sci. USA* **93**, 10200-10205.

Wyrobek, A. J., Alhborn, T., Balhorn, R., Stanker, L. and Pinkel, D. (1990). Fluorescence *in situ* hybridization to Y chromosomes in decondensed human sperm nuclei. *Mol. Reprod. Dev.* **27**, 200-208.

Zalensky, A. O., Brenenman, J. W., Zalenskaya, I. A., Brinkley, B. R. and Bradbury, E. M. (1993). Organization of centromeres in the decondensed nuclei of mature human sperm. *Chromosoma* **102**, 509-518.

Zalensky, A. O., Allen, M. J., Kobayashi, A., Zalenskaya, I. A., Balhorn, R. and Bradbury, E. M. (1995). Well-defined genome architecture in the human sperm nucleus. *Chromosoma* **103**, 577-590.

Zalensky, A. O., Tomilin, N. V., Zalenskaya, I. A., Teplitz, R. L. and Bradbury, E. M. (1997). Telomere-telomere interactions and candidate telomere bindung protein(s) in mammalian sperm cells. *Exp. Cell Res.* **232**, 29-41.